REVIEW

Early Neoproterozoic rare metal (Sn, Ta, W) and gold metallogeny of the Central Africa Region: a review

W. L. Pohl*[1], M. Biryabarema[2] and B. Lehmann[3]

The four metals of economic significance in the Central Africa or Great Lakes region, i.e. gold, tin, tantalum and tungsten, are part of one composite metallogenic system that operated about 980 ± 20 Ma. The main driving agent was peraluminous ilmenite-series granite magmatism, synchronous with intracratonic compression and associated with the final amalgamation of the supercontinent Rodinia. The granitic melts were emplaced at intrusive levels of ≥ 2 kbar (≥ 8 km); the intrusions display a variable and often advanced degree of fractionation, including abundant Sn–Ta–Li–Be–Rb–Cs pegmatites, and are associated with hydrothermal systems enriched in tin, tungsten and/or gold. Based on cumulative past production and present metal prices, gold in hydrothermal quartz veins is the major commodity, followed by tin either in rare metal pegmatites or in sheeted, hydrothermal quartz veins. Many deposits in the province occur in siliciclastic metasedimentary, or metabasaltic roof rocks above parental granites; mainly in its western part, the zone of mineralisation retracts into the granite roof. Typically in the first case, antiformal sites acted as fluid escape zones, with carbonaceous or metabasaltic rocks as chemical traps for tungsten and gold. Examples of pegmatitic and magmatic–hydrothermal deposits are presented in some detail in order to illustrate characteristics and genetic controls, and to support the metallogenic hypothesis here advanced. Impeding strategic exploration, published elements of understanding the evolution and mineralisation of the Kibara belt are contradictory and essential links are missing, foremost an understanding of the 1 Ga flare up of fertile granites. Towards solving this conundrum we suggest that the key is delamination of the mantle lithosphere and dense mafic lower crust, residual after extraction of voluminous 1·38 Ga granitic melts. During pan-Rodinian orogenic events, the Tanganyika spur of the Tanzania craton acted as an indenter whose impact caused foundering of the early Kibaran lithosphere. Consequent influx of asthenospheric heat triggered large-scale crustal melting that resulted in the tin granites. The stress state was largely compressive but possibly punctuated by short or local extensional events. The correlation of geological evolution and mineralisation substantiates the formal recognition of a Kibara Metallogenic Domain, which is composed of two units: The Mesoproterozoic (1·4 Ga) Kabanga-Musongati nickel ($\pm$copper, cobalt, platinum) province; and the early Neoproterozoic (1 Ga) Kibara rare metal and gold province that is the main subject of this paper. The present understanding of the operating metallogenic systems remains limited. Regarding the application of modern concepts and technologies, this province is drastically underexplored.

Keywords: Gold, Tin, Tantalum, Tungsten, Granite-related, Metallogeny, Africa

Introduction

A wide region in Central Africa is marked by abundant tin, tantalum, tungsten and gold deposits related to conspicuous felsic intrusions. Geographically, this giant metal province comprises Kivu and Maniema, as well as major portions of the Eastern, Kasai and Katanga

[1]Austrian Academy of Sciences, Vienna, Austria
[2]Department of Geology and Mines, Rwanda Natural Resources Authority, Kigali, Rwanda
[3]Technical University of Clausthal, Clausthal, Germany

*Corresponding author, email walter@walter-pohl.com

Published by Maney on behalf of the Institute and The AusIMM
Received 19 June 2013; accepted 10 September 2013
DOI 10.1179/1743275813Y.0000000033

Provinces of the Democratic Republic of the Congo (DRC). It also includes Burundi and Rwanda, and marginal territories of Tanzania and Uganda. Estimates of past cumulative production converge at 800 000 t cassiterite (SnO_2), 30 000 t columbite ($\sim$50% Ta_2O_5), 30 000 t wolframite (WO_3) and 600 t gold. At times, bismuth, molybdenite, beryl and amblygonite were byproducts.

The region is geologically known as the intracontinental Mesoproterozoic Kibara belt (Fig. 1; Cahen *et al.*, 1984) and as the Kibara Metallogenic Province (Pohl, 1987, 1994), the proper noun being derived from the Kibara Mountains in Katanga (Kokonyangi *et al.*, 2005). Use of the term has been extended to designate collectively other (Kibaran) belts of comparable age and lithologies in western and southern Africa such as the Irumide belt (De Waele *et al.*, 2003) that lack, however, the metal endowment of the Kibara belt itself. Only in Natal and Namaqualand, are there coeval pegmatites of possible economic significance (Thomas *et al.*, 1994).

For decades, scientific fieldwork, exploration and mining development in the Kibara belt was restricted to its marginal parts. After a prolonged period of armed conflicts in the region, peace is returning. Mining can be one important element of rehabilitation and development.

Modern concepts and technologies have increasingly been applied to investigations of the Kibara belt and its mineral systems, but there has not been an evaluation of historic and recent data aimed at a unifying metallogenic overview. This paper attempts to fill this gap.

Geological background

The Congo Craton was assembled from Archaean nuclei by multiple Palaeoproterozoic orogenies, and during the Mesoproterozoic, was welded by the Kibara belt to the Tanzania Craton and the Bangweulu microcraton (Fig. 1). The Kibara belt is built of Kibara Supergroup basin fill that is predominantly sedimentary siliciclastic, with very rare carbonates and small volumes of bimodal volcanic rocks and more common mafic sills of intraplate character; the total thickness is estimated at >10 km. There is, however, no uncontested basin-wide lithostratigraphic scheme. Probably, several sedimentation centres evolved individually, which resulted in the formal recognition and naming of individual sub-basins and a proposal that the unifying term 'Kibaran' should be discontinued (Fernandez-Alonso *et al.*, 2012; Tack *et al.*, 2010). Near the passive basin margins, for example in SW Uganda, thick quartz conglomerate fans mark alluvial entry points into a generally shallow sea. Quarzite, sandstone, slate and schist are the most common rocks. Within the basin, graphitic shale and dolomite horizons serve as markers in regional mapping (Brinckmann *et al.*, 1994). Deep water black shale and sandstone turbidites, often studded by pyrite cubes, overlying shallow water sediments with ripple marks characterise the Rwanda–Uganda tungsten belt. The apparent continuity of vertical sections masks unconformities and temporal breaks (Kokonyangi *et al.*, 2007). Late orogenic siliciclastic sub-basins such as higher conglomeratic sections of the Itombwe in South Kivu have a molasse-like character (Cahen *et al.*, 1984). Ophiolites and accretionary magmatic arcs are unknown; subduction-related magmatism, however, is possibly indicated by gabbro to diorite lithologies in Mitwaba, DRC (Kokonyangi *et al.*, 2005).

Orogenic structures are dominated by upright or moderately vergent folds with vertical to steeply inclined axial planes. Cross-section shortening by folding and thrusting is near 50%. Syntectonic S-type batholithic granites (G1 and G2 according to Cahen *et al.*, 1984), which occupy anticlinoria and are often foliated, date peak compression (the Kibaran tectono-thermal event: Cahen *et al.*, 1984) to a minimum of 1·38 Ga (Tack *et al.*, 2010; De Waele *et al.*, 2008). The S-type granite batholiths were preceded by the >500 km long Kabanga–Musongati belt of layered mafic–ultramafic intrusions with magmatic and lateritic Ni deposits (Maier *et al.*, 2008). The belt parallels the border of the Tanzania Craton, but intrudes Kibaran sedimentary rocks. With a crystallisation age of 1403 ± 14 Ma (SHRIMP U–Pb zircon age: Maier *et al.*, 2007) the intrusions mark a pre-orogenic extensional phase tapping the mantle during Kibaran basin formation. Later thrusting characterises the contact between Archaean NW striking granite–greenstone rocks of the Tanzania Craton and the north-trending structural grain of the Meso- to early Neoproterozoic Kibara belt (Kabete *et al.*, 2012).

Two separate phases of metamorphism affected Kibaran sedimentary rocks. An earlier phase centred on the large syn- to late-tectonic G1 and G2 granite batholiths reached intermediate pressure (4–5 kbar or ca. 16–20 km depth) and intermediate temperature (500–600°C) marked by staurolite-kyanite-sillimanite in metapelites and by incipient melting exhibited in migmatites; high thermal gradients are implied by small distances from slate to high-grade schists. A later metamorphic phase, related to 1 Ga granite magmatism is characterised by an aureole of andalusite in metapelitic country rocks, which indicates lower pressures and shallower levels of emplacement that are supported by the occurrence of spodumene in associated rare-metal pegmatites ($\geq$2·5 to $\leq$4 kbar or 10–16 km depth according to Lehmann *et al.*, 2013). Large areas of the Kibara belt expose this level, where earlier basement, Kibaran metasedimentary rocks and granites are interlayered. In both metamorphic settings, cleavage or schistosity is weakly developed or absent. In regions with poor outcrops, the boundary between amphibolite-facies Kibaran metasedimentary rocks and comparable Palaeoproterozoic metamorphic basement rocks is not easily established.

The Kibara belt forms the eastern margin of the Congo Craton but the actual contact is largely buried beneath younger sediments of the Phanerozoic Congo Basin (Fig. 1). The belt can be followed for about 1800 km from SW to NE with fold axes striking north to northeast, roughly parallel to the Tanzania Craton boundary. In the extreme north folds appear to bend to the west along the Uganda Craton border apparently forming an orocline. The Mesoproterozoic plate tectonic setting of the Kibara belt is unresolved; but an intracratonic position is widely accepted. Relating to the G1 and G2 granites, the involvement of a large igneous province at 1·38 Ga is suggested by Tack *et al.* (2010). Kokonyangi *et al.* (2005), however, propose a supra-subduction setting for the Mitwaba area in Katanga and, implicitly, for the whole belt.

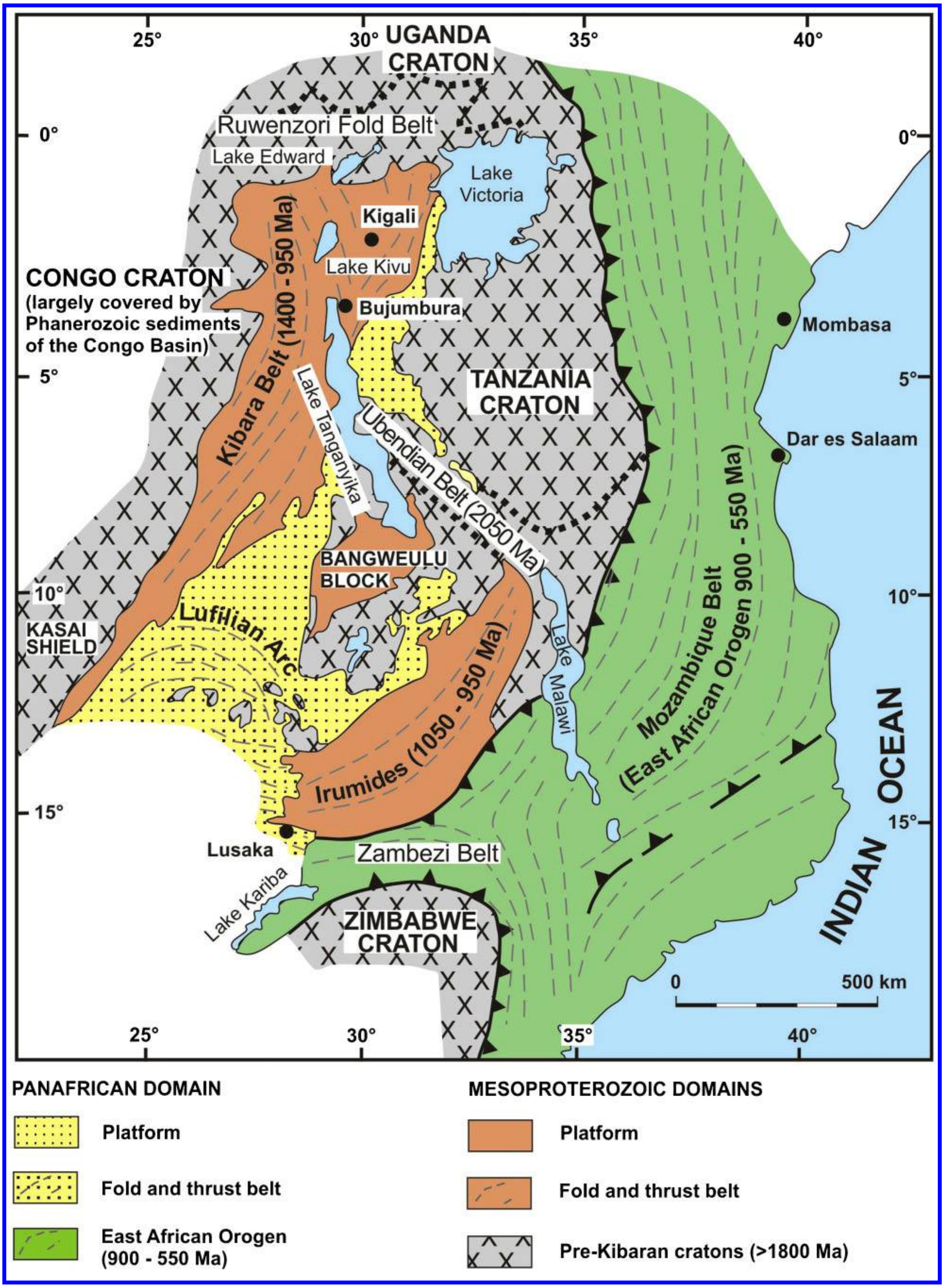

1 Structural and geographic setting of the Kibara belt in the Central Africa region between the Congo craton to the west, and the Tanzania craton and the Bangweulu micro-craton to the east and southeast, respectively (modified from Cahen *et al.*, 1984)

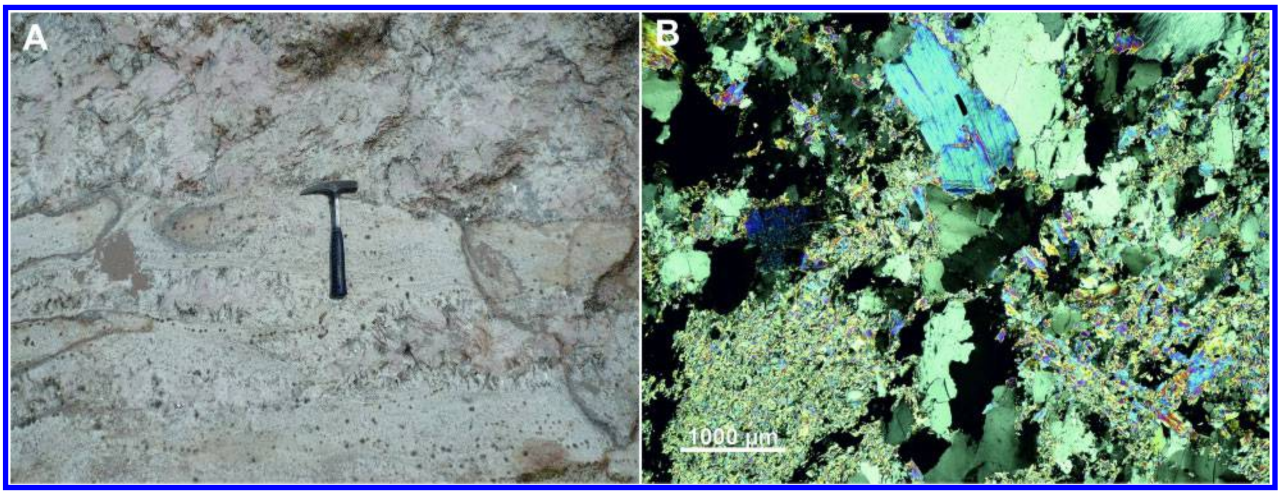

2 (A) Convolute structure of granite–aplite–pegmatite outcropping between two Sn–Ta mines in the Gatumba district, Rwanda (for location compare Fig. 5). The granite and aplite consist of alkalifeldspar leucogranite with disseminated almandine–spessartite garnet (dark spots); the pegmatite domains are characterised by large booklets of muscovite, quartz and coarse-grained alkali feldspar. Dark rims of aplite–granite schlieren indicate resorptive reactions. (B) Photomicrograph (crossed nicols) of muscovite–quartz rock (endogreisen) from a sheared domain of the same locality as above. Part of the black patches are opaque ore minerals, others are holes. This sample has a bulk-rock content of 31 ppm Bi, 160 ppm As, 281 ppm Sn, 12 ppm W, and 32 ppb Au, interpreted as a hydrothermal signature

At about 1 Ga, renewed compressive deformation in a different stress field and flooding by collisional granites that include fertile highly differentiated members (i.e. tin granites, as defined by Lehmann, 1990) are related to gold and rare metal mineralisation throughout the Kibara belt. The $\sim$1 Ga tectono-magmatic events in the Kibara belt coincide with the final stages of the assembly of supercontinent Rodinia (the pan-Rodinian orogenic events of Li *et al.*, 2008). Published reconstructions of Rodinia fail, however, to illuminate the tectonic evolution of this region.

The Kibaran tin granites (also called G4 granites: Cahen *et al.*, 1984) are typically equigranular, non-foliated and leucocratic. They consist of quartz, microcline, albite and muscovite, with accessory apatite, garnet, zircon and tourmaline; their generally subalkaline to peraluminous modal and geochemical character is a function of the variable degrees of differentiation (Lehmann and Lavreau, 1988). Compared to common granites, the G4 granites are enriched in Li, Rb, Cs, U, Cr, B, Ga, Ge, Sn and Pb (n=50; De Clercq, 2012). Profuse boron, but little fluorine characterises the volatile phase. Many G4 granites exhibit aplitic and pegmatitic textures, and miaroles or veinlets of tourmaline and quartz or amethyst. Rarely, exposures display the transition from the parental granite to aplite-pegmatite systems (Fig. 2A and B). Post-solidus hydrothermal alteration (albite, muscovite/sericite, tourmaline, kaolin) and poor exposure caused by deep weathering are characteristic, and therefore no detailed maps of single intrusions nor of regional G4 granite distribution, are available. G4 granite melts intrude Palaeoproterozoic basement, the older batholithic granites and Kibaran metasedimentary rocks. Emplacement was preferentially in antiformal structures controlled by tightening of previous folds, by cross-folding and thrusting. Outliers of G4 granites in near-field pre-Kibaran basement are known, for example at the Mashonga gold placers in Uganda (Pohl and Hadoto, 1990). Tack *et al.* (2010) provide a SHRIMP U–Pb zircon age of 986$\pm$10 Ma for a sample of the Kazika G4 granite (Itombwe, DRC), which confirms previous Rb–Sr dating (976$\pm$10 Ma; Cahen *et al.*, 1984). Initial zircon ^{176}Hf/ ^{177}Hf ratios (εHf$_{(t)}$) ranging from -3 to -19 indicate a considerable heterogeneity of the magma and its source, which was dominated by older crust and likely included mantle components. Further to the West in the DRC, G4 granites display geochemical characteristics relating to the mantle, such as high Sr concentrations and low initial Sr-isotope ratios (Lehmann and Lavreau, 1988). The ensialic nature of these ilmenite-series granites is not in doubt, however, and there is no evidence for an accretion and/or subduction-related setting. This distinguishes the G4 granites from the type of intrusions related to Sn–W–Au systems described by Lang and Baker (2001).

Deep and intensive weathering is the key for the economic feasibility of a large number of mines in the region. Enriched gold in oxide zones and eluvial placers of cassiterite, columbite and wolframite are all the product of supergene alteration. Lateritic regolith formation is associated with the African Erosion Surface that formed between 180 and 30 Ma (Burke and Gunnell, 2008). Mainly by tectonic activities after 30 Ma, such as rifting, the surface was warped, dissected and partly eroded. In an E–W profile of the region considered here, the African Erosion Surface occupies low elevations from Lake Victoria westwards (hosting the giant Musongati Ni-laterite resources) but is uplifted to 1·7 km on the shoulders of the Western Rift, where supergene enrichment ore bodies tend to be shallow, partly eroded and less concentrated. In the central Congo Basin, the African Erosion Surface is buried beneath young terrestrial sediments that include a Cretaceous lacustrine succession (Cahen, 1954).

For the major part of the Kibara belt, geological overview maps are available (e.g. Fernandez-Alonso *et al.*, 2007) but detailed maps based on ground work are rare. Most published maps have a provisional and overview character (RMCA, 2005a, 2005b). In the

1980s, the Bureau de Recherches Géologiques et Minières (BRGM, Orléans) published mineral deposit maps covering the region (e.g. NN, 2000; Baudin *et al.*, 1982; Ziserman *et al.*, 1983), some of which approach the character of metallogenic maps by imparting some genetic information (Baudin *et al.*, 1982).

Early Neoproterozoic metallogeny of the Kibara Belt

The Kibara metallogenic domain comprises two fundamentally different units:

(i) the Mesoproterozoic (1·4 Ga) Kabanga-Musongati nickel ($\pm$copper, cobalt, platinum) province; and

(ii) the early Neoproterozoic (1 Ga) Kibara rare metal and gold province that is the main subject of this paper.

Until now, small and scattered mineralisation of iron oxides, iron sulphides and industrial minerals such as andalusite, kaolin, quartz and talc remained economically insignificant (Pohl, 1987, 1994).

The 1 Ga Kibara rare metal and gold province (Fig. 3) comprises a large number of G4 granite related deposits that include pegmatitic and magmatic–hydrothermal types. Endogranitic ore deposits such as breccia pipes, cupolas of albitite or greisen have not been described. Apart from mineralisation developed in older (G1 or G2) granite reported from the Congo (Cahen, 1954), most ore is exogranitic and occurs in the form of pegmatites and quartz veins (Varlamoff, 1972). This may be a function of the predominance of boron over fluorine as a fluxing compound because the second tends to induce endogranitic greisen and disseminated ore (Lehmann *et al.*, 2000), which is unknown in the Kibaran. Boron-rich volatiles, in contrast to fluorine, typically mark overpressured granite systems that lead to expulsion of residual liquids and fluids. Consequently, the majority of important ore deposits consist of clusters of pegmatite dykes or of quartz veins emplaced in the roof of parental tin granites. The source granites display many common features as described above, but differ in the depth of emplacement, the nature of intruded rocks, and most importantly, in the deposit type and the metal(s) produced.

Typically in the Kibara belt, pathways and traps for pegmatite melts, or for metalliferous hydrothermal fluids, were low-pressure hinge zones of tightening anticlinal folds with axial planes or cleavage planes on the flanks of folds as feeder and break-through structures. The compressive stress field was rotated compared to the Mesoproterozoic main deformation and produced fold axes and thrusts cutting earlier folds at sharp to orthogonal angles. Outcrop patterns created by fold interference are visible on geological maps; resulting highs often determined the location of tin granite cupolas or ridges and associated deposits.

The following section provides a general characterisation of the deposit types and a closer inspection of individual deposits that have received some more recent scientific or commercial attention and can serve as models (Table 1).

Tin and tantalum in pegmatites

An important part of the tin and all of the tantalum production of the region is sourced from rare element lithium–cesium–tantalum (LCT) pegmatites with some by-production of beryl, amblygonite, bismuth, molybdenite and wolframite.

Kibaran LCT pegmatites are derived from G4 magma bodies. They crystallised from highly fractionated hydrous residual melt batches enriched in volatiles and incompatible trace elements. This is illustrated by pegmatitic schlieren occurring in many G4 granite exposures. A continuous line of increasing fractionation connects relatively primitive and mineralised pegmatites (Hulsbosch *et al.*, 2013). The regional zoning of variably differentiated pegmatites centred on parental granites and with the mineralised ones injected farthest from the source as proposed by Varlamoff (1972) is not always well developed. In many cases, the increasing fractionation is only recorded in pegmatite pockets preserved within the parental granite. Some, but not all of the rare metal pegmatites are internally zoned. Typically in the former, a quartz core is surrounded by a zone of large crystals of spodumene, amblygonite, beryl and nests of quartz and microcline that hosts much of the ore minerals. At one site in northern Burundi, snake-like coils of spodumene laths enlace the quartz core. Marginal zones comprise coarse-grained pegmatite in which microcline dominates. In contact with metapelites, a fringe of muscovite is formed (Varlamoff, 1972) and tourmaline is widespread in pelitic country rocks.

After a long period of disinterest by science and mining, Kibaran LCT pegmatites again attracted attention, when in recent years, Gatumba Mining Concessions and Kivu Resources decided to explore the hard-rock potential of the formerly important Gatumba mining district (Rwanda). Since 1928, about 20 000 t of cassiterite and 4000 t of columbite–tantalite (referred to as coltan) concentrate had been produced, mainly from alluvial, eluvial and colluvial placers, and from soft regolith ore with a combined average grade of 0·5 kg m^{-3}. By-production of several hundred tonnes each of bismuth and beryl is recorded. In 2008, considerable open pit hard rock tin–tantalum reserves of one dyke were defined by drilling (Lehmann *et al.*, 2013: 26 Mt at 153 g/t Sn, 70 g/t Ta and 82 g/t Nb). At present, the mine is in the construction phase. Support of the project by RMCA (Royal Museum for Central Africa) facilitated renewal of scientific investigations (Dewaele *et al.*, 2011, Hulsbosch *et al.*, 2013).

At Gatumba, some 130 steeply dipping pegmatite dykes invade a suite of metasedimentary rocks (pelitic siltstones and sheets of sand deposited in tidal flats) and 150–200 m thick mafic sills (i.e. dolerite), over a N–S distance of 20 km. The structural setting is a subsidiary antiform on the flank of a large and narrow synform between two broad anticlinoria occupied by batholithic granites (Fig. 4). In the southern part of the district, the fertile sub-intrusion that sourced the pegmatites is exposed (Fig. 2A); most likely, it forms a buried ridge trending S–N and underlying the pegmatite swarm. Individual pegmatites reach a thickness of 30 m and a length of 2400 m. Minor Sn–W quartz vein deposits occur distally to the pegmatites.

A generalised cross-section of the pegmatites shows a fine-grained tourmaline-rich chilled margin, followed by inwardly coarsening microcline, muscovite and quartz. Increasing albite content is associated with columbite, amblygonite, spodumene, apatite, beryl and some pyrite. A quartz core is rare; often, quartz veins and veinlets

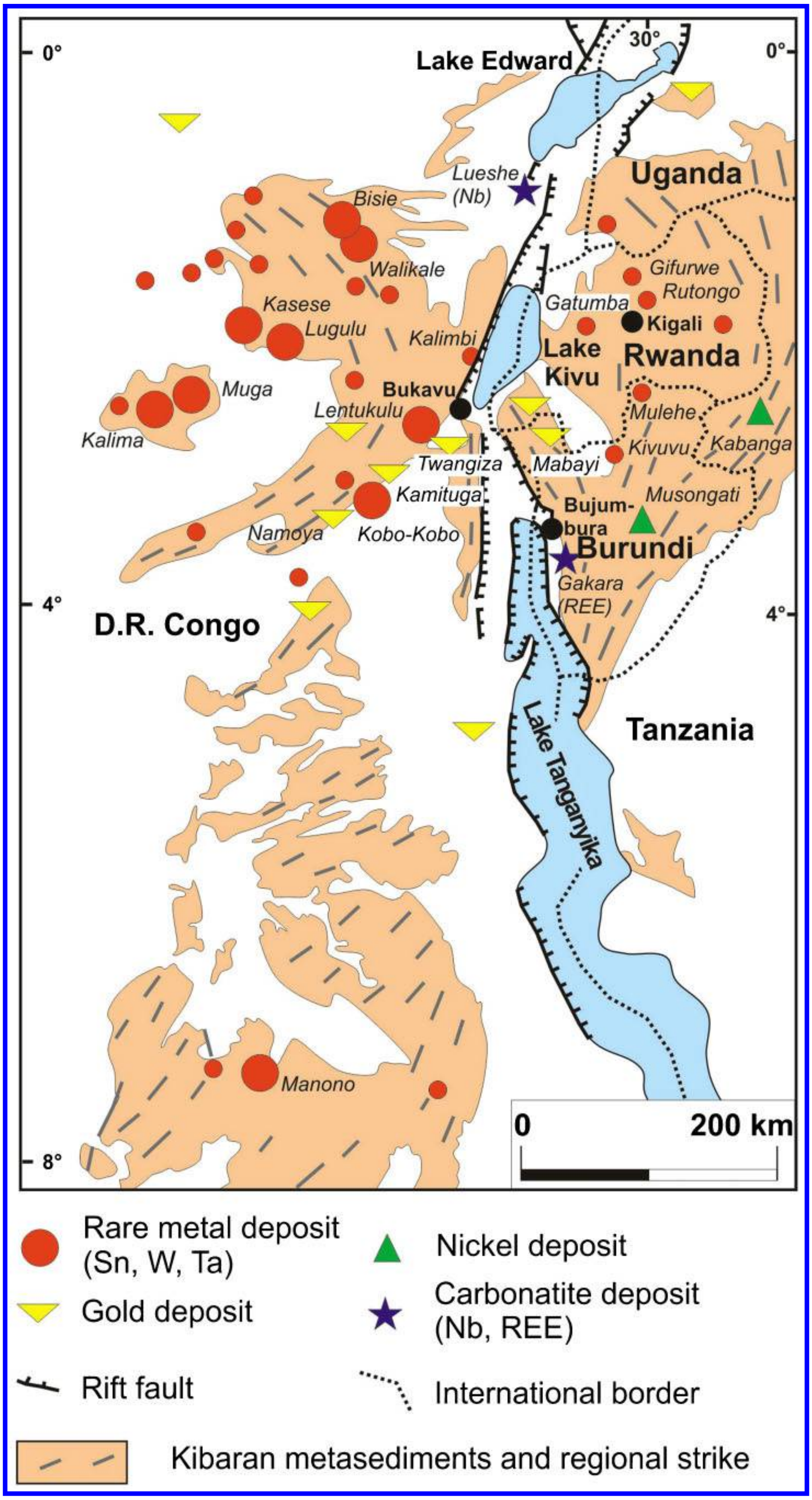

3 Major ore deposits in the Kibara metallogenic domain of the Central Africa region (modified from A. Blanchot in Baudin *et al.*, 1982). Shading marks metasedimentary and granite terrains affected by the Kibaran orogeny (~1·37 Ga). The Ni deposits (apex) occur in or above ultramafic intrusions related to early intracratonic rifting at ~1·4 Ga. Gold (triangles) and Ta, Sn and W deposits (dots; larger dots signify economically outstanding sites) are related to ~986 Ma granite magmatism. Nb and REE deposits (stars) along the present-day Western Rift formed during late Neoproterozoic to Cambrian extensional tectonics

Table 1 Kibaran pegmatitic and magmatic–hydrothermal deposits: general information on examples presented in this paper

Name	Gatumba	Manono	Rutongo	Bisie	Nyakabingo	Ruhembe	Twangiza
Location	Open pit mining district 70 km W of Kigali, Rwanda	Opencut mines in northern Katanga, DR Congo	Underground mining district 25 km N of Kigali, Rwanda	Underground diggings ~130 km west of Goma, North Kivu, DR Congo	Underground and former open cut mines ~40 km NW of Kigali, Rwanda	Artisanal gold diggings in wide area of NW Burundi ~100 km north of Bujumbura	Industrial opencut gold mine ~40 km SSE of Bukavu town in South Kivu, DR Congo
Type	Tin and tantalum in lithium–caesium–tantalum (LCT) pegmatite dykes	Tin and tantalum (plus spodumene potential) in giant LCT pegmatite	Tin in fields of magmatic hydrothermal sheeted quartz veins	Polymetallic hydrothermal tin and copper, a hitherto unknown deposit type in the region	Tungsten in hydrothermal quartz veins hosted by black shales in dome shaped anticline	Hydrothermal gold quartz veins, closely related to LCT pegmatites, or in auriferous iron oxide breccias	Hydrothermal gold quartz veins in sediments along the crest of an anticlinal structure
Production	Historic 20 000 t cassiterite plus 4000 t Ta-rich columbite; present production <10 t/month	Historic 180 000 t cassiterite plus 9000 t Ta-rich columbite	Historic 50 000 t cassiterite; 10% alluvial, 25% eluvial, 65% primary; present production not published	Not known, but reportedly for several years, produced most of the annual national (DRC) cassiterite export	Historic 8000 t (?) wolframite; present production <10 t/month	Probably <1000 kg per annum; the area is the source of most gold produced in Burundi	Previous artisanal production of unknown tonnage; since 2012, 10 000 ounces of gold per month
Resources, Reserves	New mine NI 43-101 compliant 26 Mt open pit ore reserve	Not known or not published	Not known or not published	Not known or not published	Not known or not published	Not known or not published	Reserves estimated according to NI 43-101
Grade	Historic 0·5 kg m^{-3}; new mine 26 Mt @ 153 g/t Sn, 70 g/t Ta, 82 g/t Nb	Not known or not published	6 kg/t cassiterite	Not known, artisans reported a large mass of solid cassiterite	Not known or not published	Not known or not published	oxide ore 17·9 Mt @ 2·3 g/t Au; sulphide ore 89·6 Mt @ 1·5 g/t Au
Main sources	Dewaele *et al*., 2011; Lehmann *et al*., 2013	Bassot and Morio, 1989	De Clerq, 2012	Alphamin Resources Co. website http://alphaminresources.com	De Clerq, 2012	Brinckmann *et al*., 2001	Banro website http://www.banro.com
Figures	2A, 2B, 4		5, 6		7	8A, 8B	
Note	Hard rock mine in construction	Present activity not known	Active mining	Artisanal eldorado discovered about 2000; since 2010 exploration; drilling proved elevated Sn, Cu, Ce, Ag, Zn and Pb tenors	Active artisanal mining	Active artisanal mining	Mine started producing in 2012; in the whole region, very lively artisanal mining

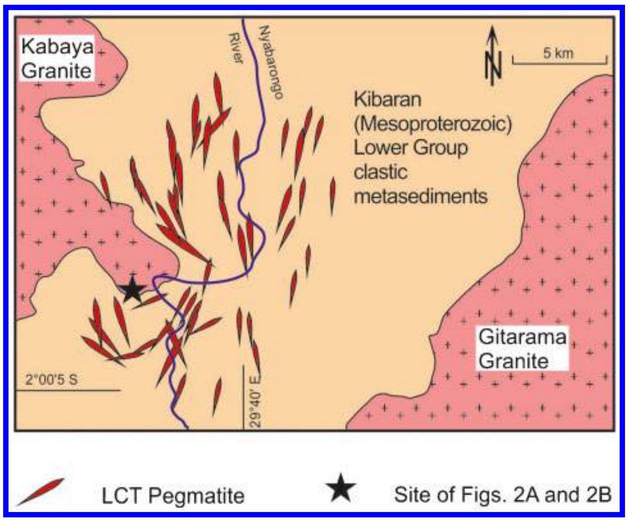

4 Sketch map of the Early Neoproterozoic pegmatite dyke swarm in the Gatumba tin–tantalum mining district, Rwanda. Near Nyabarongo River (locality marked by star), an outcrop displays banding of pegmatite, microgranite and aplite, typical for the carapace of an apical tin granite (see Fig. 2A and B). Most likely, this is the parental sub-intrusion to the pegmatite dykes

rich in green muscovite take its place. Post-solidus replacement pockets and masses of albite, sericite and muscovite occur at random in the pegmatites. Coarse hydrothermal muscovite is correlated with massive cassiterite in the greisen (i.e. muscovite) pockets (Fig. 2B), independent of columbite minerals that formed from the melt phase and are disseminated (Dewaele *et al.*, 2011). Hydrothermal alteration extends into the mafic host rock and is marked by formation of biotite and the bluish-black lithian amphibole holmquistite.

Heavy mineral concentrates from Gatumba pegmatites consist of cassiterite, ~15% columbite–tantalite group minerals, microlite, tapiolite, uraninite, uranmicrolite, wodginite, ilmenite, rutile, wolframite and zircon (Lehmann *et al.*, 2013). Columbite group minerals vary from columbite-(Fe) to columbite-(Mn), and evolve to tantalite-(Fe) or tantalite-(Mn). Minor and trace element contents of interest comprise bismuth (159±88 ppm, max. 0·6% Bi), arsenic 100–600 ppm (367±166 ppm As) and uranium 150–1400 ppm (1230±1520 ppm, max. 1·3%U) (Lehmann *et al.*, 2013). In individual pegmatite dykes and across the Gatumba district, mineralogical and chemical composition of the ore is highly heterogeneous.

The first precise U–Pb ages of columbite in Kibaran pegmatites (NW Burundi) yielded a pooled age of 965±7 Ma and a lower intercept age of 620±20 Ma (Romer and Lehmann, 1995). U–Pb dating of columbite from Gatumba results in scattered apparent ages; a selection of geologically reasonable data provides an upper intercept age range from 936±14 to 974+8·2/−8·3 Ma (Dewaele *et al.*, 2011). The older dates correspond within error to the columbite age reported by Romer and Lehmann (1995), and to the zircon age of 986 Ma for the G4-granite dated by Tack *et al.* (2010). Younger columbite and muscovite ^{40}Ar–^{39}Ar ages (Dewaele *et al.*, 2011) are attributed to disturbance triggered by the break-up of Rodinia at ~750 Ma (Kampunzu, 2001), and pan-African (650–550 Ma) far-field effects, already recognised by Cahen *et al.* (1984).

Manono in Katanga, DRC, is a classic example of a zoned, complex LCT pegmatite. Manono is probably the world's largest pegmatite deposit of cassiterite and tantalum minerals mined to date. Cumulative production since 1919 is reported as 180 000 t of cassiterite concentrate including 9000 t (5 wt-%) of columbite group minerals (Bassot and Morio, 1989). The pegmatite contains an untested hard rock resource of spodumene.

Manono is a giant pegmatite, exposed on the surface for 12 km in length with a width of 50 to 800 m. As a subhorizontal sheet, probably injected parallel to the roof of its parental granite, it displays asymmetric bottom-to-top differentiation. Based on few actual observations, its thickness is estimated at 200–300 m (Bassot and Morio, 1989). Country rocks are metasediments (phyllite, quartzite, chert) and greenstone, with steep schistosity planes. Near the pegmatite, these rocks are hydrothermally altered by tourmalinisation, silicification and the formation of Li-mica. Among several different granites in the area, conspicuously red leucocratic granite is probably related to the pegmatite. The granite displays muscovite, tourmaline aggregates and garnet. It is S-type, peraluminous, depleted in REE, but with a pronounced negative Eu anomaly, and plots as syn-collisional in Rb–Hf–Ta or Rb/Yb+Ta plate tectonic discrimination diagrams (Günther and Ngulube, 1992).

The Manono pegmatite is strikingly zoned. Of nine mineral assemblages differentiated in the open pit, yellowish albitite with the highest Sn and Ta concentration, huge crystals of microcline, blue tourmaline (elbaite), metre-long vertical laths of spodumene and metasomatic greisen (coarsely crystalline mica pockets rich in cassiterite) with zinnwaldite are noteworthy, as is the absence of a quartz core. Weathering to 80 m depth below surface produces kaolin-bearing assemblages.

Magmatic–hydrothermal tin and tungsten vein deposits

Tin and tungsten ore is extracted from quartz veins and their immediate contact zones with reactive host rocks, commonly metapelites and meta-arenites. The quartz veins mark fluid escape zones above granite cupolas or emanate from pegmatites as at Musha (Fig. 5). Anticlinal structures of the Kibaran roof rocks provide traps, probably a few hundred to a maximum of 1000 m above the apex of the intrusive contact. Host rocks are different for the large tin and tungsten vein deposits: Brittle quartzites are the preferred host for tin whereas tungsten is concentrated in thinly bedded carbonaceous sandstone and black shale alternations.

Tin and tungsten (and gold) vein deposits share many features including paragenesis, hydrothermal wall-rock alteration and tectonic control. At most deposits, either tin or tungsten is concentrated although often with traces of the subordinate metal (and of gold); nevertheless, some deposits are known in the Congo where cassiterite and wolframite were produced in equal quantities (Cahen, 1954).

One of the largest tin districts of the Central Africa region, reasonably covered by more recent scientific sources, is the Rutongo mining district in central Rwanda (Fig. 5). Hundreds of sheeted quartz-cassiterite veins form several distinct fields on the eastern flank of an anticline, which is cut by a major west-vergent thrust fault. In its hanging wall, the vein fields are located by

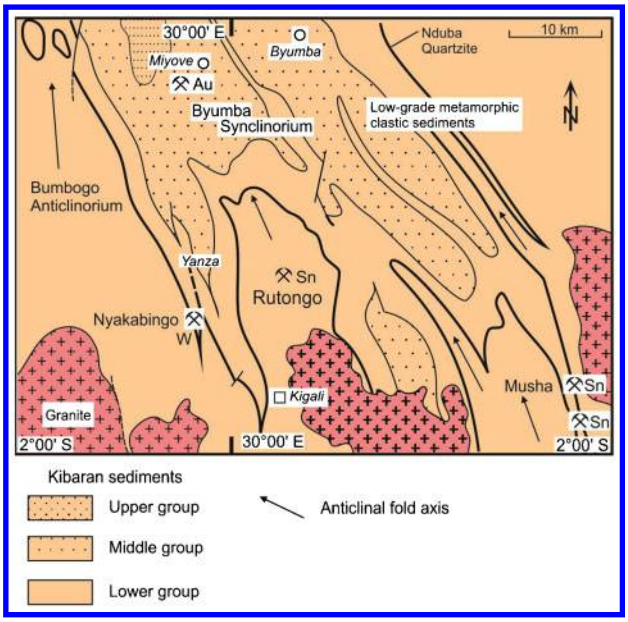

5 Pegmatitic tin (Musha) and magmatic–hydrothermal vein deposits of tin, tungsten and gold in the metasedimentary roof of Early Neoproterozoic (~986 Ma) tin granites in central Rwanda. Miyove is a small artisanal mine working a steeply dipping gold quartz vein within a wide zone of alluvial mining (Ziserman *et al.*, 1983). Thick lines denote the distinctive quartzite marker bed of the Nduba Formation. Arrows trace anticlinal fold axes and indicate their plunge direction, away from the complex granite batholith in the south

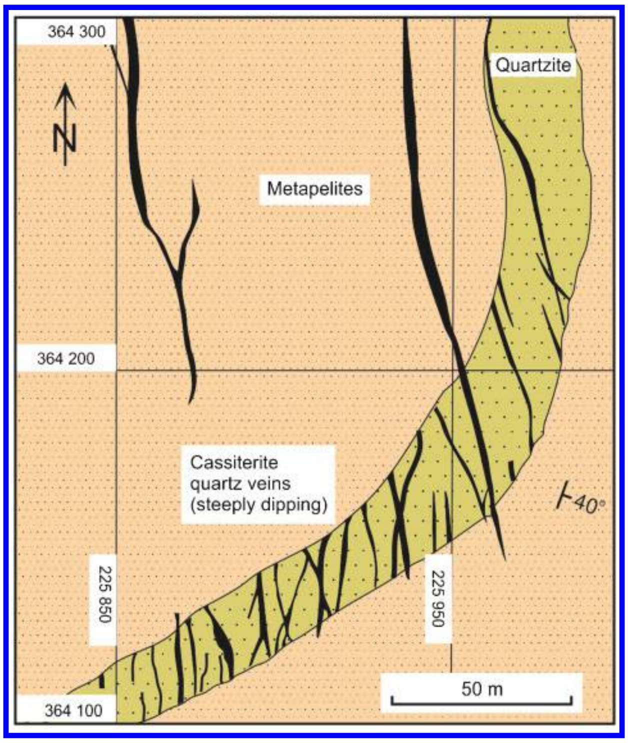

6 Geological map of 1736 m underground mining level in Rutongo tin mine, Rwanda, showing closely spaced parallel (sheeted) quartz–cassiterite veins (black) hosted in brittle quartzite. Coordinates in metres

the intersection of a broad (1·5 km), elongated (6 km) fluid escape zone with brittle quartzites in secondary cross-cutting (F3) anticlines. The core of the (F1–F2) anticlinorium is intruded by the Kigali G4 granite. A fine-grained leucogranite with miaroles and veinlets of muscovite, tourmaline and quartz is best exposed about 5 km south of the mines. Since 1930, five mines at Rutongo produced a total of about 50 000 t cassiterite concentrate (10% alluvial deposits, 25% eluvial and 65% primary). The average grade of primary Sn ore in quartz veins is reported at 6 kg/t. Much of the ore, however, was extracted from nugget-like high-grade pockets of cassiterite, muscovite and tourmaline that occur adjacent to kaolinised and sericitised host metapelite. In the main quartz fill, cassiterite and muscovite occur in fractures but often, this material is not economically exploitable. Host quartzites are silicified and glass-like, whereas alteration of metapelites is characterised by disseminated fine needles of tourmaline and some biotite (De Clercq, 2012).

Cassiterite, white massive quartz, kaolin-altered feldspar, muscovite, rutile and tourmaline precipitated first in the paragenetic sequence, followed by grey quartz and sulphides (arsenopyrite, pyrite, chalcopyrite, galena). In the Kalima region (Maniema, DRC), additional sphalerite, stannite, bismuth and molybdenite are reported, and at Mitwaba, beryl and feldspar (Cahen, 1954). The gold found in cassiterite placers was probably liberated by oxidation of the sulphides. Although underground mining at Rutongo (Fig. 6) operates over 100 m below the base of the regolith, hematite–goethite coatings on joints are common.

Fluids precipitating cassiterite and quartz were aqueous–gaseous with a low to moderate salinity (6–15 mass-% NaCl eq.) and a minimal temperature of 330°C (De Clercq, 2012). The gas phase is composed of CO_2 (50–78 vol.-%), N_2 (11–40 vol.-%) and smaller amounts of CH_4 (10–15 vol.-%). $\delta^{18}O$ of hydrothermal fluid (water) in equilibrium with quartz and cassiterite is 8–9‰, whereas δD displays a wide scatter. Na is the dominant cation in solution, with lesser amounts of K, Li and Cs; Cl is the main anion (De Clercq, 2012). The magmatic–hydrothermal nature of the fluids is well supported by these data; the gas phase suggests interaction of the fluids with organic-rich metasedimentary rocks.

Bisie tin mine near Walikale in North Kivu (DRC) appears to be a newly discovered polymetallic type of tin deposit within the Kibara metal province. About 10 years ago, it was found and developed by artisans and quickly became the country's largest producer of cassiterite. Along a ridge formed by sediments in contact with a tin-bearing granite occupying a depression, characteristic for the arena morphology common in SW Uganda, mineralisation occurs along 1·5 km strike. An ore shoot measuring 15×8 m of nearly solid cassiterite was opened up by artisanal miners 80 m below surface. In the paragenetic succession, early cassiterite is reportedly followed by massive pyrite–arsenopyrite, which is replaced by chalcopyrite and bornite, and lead and zinc sulphides. Extensive chlorite alteration affects the wall rocks. The company exploring the deposit since 2010 compares the setting with San Rafael in Peru (Alphamin Resources Corporation, 2013), a giant vein and breccia Sn–Cu deposit that hosts over 1 Mt of contained tin metal at an average grade of 4·7% Sn (Pohl, 2011). Alphamin reports 2400 m of drilling that resulted in significant tenors of Sn, Cu, Ce, Ag, Zn and Pb. Not far from Bisie, gold placers and veins are worked by artisans.

The style of Kibaran magmatic–hydrothermal tungsten deposits is best studied in the Rwanda–Uganda tungsten belt, from which originated a total production of ~25 000 t WO_3. Over 100 km from south to north, four larger deposits are arranged along the Bumbogo anticlinorium: Nyakabingo-Shyorongi (Fig. 5), Gifurwe, Bugarama, and Kirwa in Uganda. Anticlinal compressive tectonic control, proximity of large faults, low-grade metamorphic host rocks rich in graphite (1–4% C), dense quartz veining and a peculiar paragenetic sequence (see below) are common characteristics (De Clercq, 2012).

The Nyakabingo tungsten mine at Shyorongi near Kigali (Rwanda) is worked underground. Orebodies are sets of thin quartz veins that occur within a domal structure formed by the rectangular intersection of pan-Rodinian (F3) crossfolds with the main Kibaran (N–S) fold axes. The spatial arrangement of cross-cutting quartz veins reflects structural control by a compressive stress regime (De Clercq, 2012; Pohl, 1994; Fig. 7). The near-horizontal disposition of early bedding-parallel veins indicates that initially fluid pressures were higher than the vertical lithostatic stress.

The paragenetic sequence of wolframite–quartz veins displays three very different stages – first, precipitation of quartz, scheelite, and massive, tabular wolframite; second, the near complete replacement of scheelite by secondary wolframite (reinite); and third, a minor sulphide phase.

The injection of fluids into veins initiated host rock alteration marked by a wide pervasive zone of dispersed euhedral tourmaline needles, a more proximal biotite zone and in some cases, bleaching adjacent to veins. Reactions with metapelite produced kaolinite pockets and several centimetre-thick coarse muscovite fringes at vein contacts and inside the veins around fragments of host rock. An early oxide phase (1) precipitated euhedral massive wolframite (ferberite 1), bipyramidal scheelite crystals and some molybdenite, arsenopyrite, rutile and pyrite within the main quartz fill. Phase (2) wolframite (ferberite 2) is dispersed in proximal host rock or in the main quartz; it replaces earlier scheelite and is remarkably porous and friable, displaying boxwork texture, and is composed of microscopic fibres. For the sulphide phase (3) only microscopic evidence demonstrates the presence of chalcopyrite, galena, cosalite, native bismuth, bismuthinite and siderite (De Clercq, 2012). Late impregnations of hematite and goethite are ubiquitous in veins, as are minor oxidised tungsten minerals such as ferritungstite and anthoinite.

Phase (2) is striking because the iron metasomatism of scheelite may be related to the formation of myriads of cube-shaped cavities that characterise the dark host rocks exposed in the mines (Pohl and Günther, 1991). The cavities originated by dissolution of diagenetic pyrite. For solubilising iron and sulphur from disseminated pyrite, the host rocks must have been pervasively flooded by a pulse of acidic and reduced fluids. Isotopic investigations of phase (1) and phase (3) sulphur should expose the sedimentary or magmatic source. Probably, fluid flooding of the host rocks took place before opening of the transverse structures that drained the overpressured structural trap (Fig. 7).

The tungsten-bearing fluid of phase (1) was aqueous–gaseous with a low to moderate salinity (1–14 NaCl eq. mass-%) and a trapping temperature between 250 and 500°C (De Clercq, 2012). The gas phase of inclusions is composed of CO_2 (50–90 vol.-%), N_2 (5–40 vol.-%) and minor amounts of CH_4 (1–10 vol.-%). Dissolved cations are dominantly Na, Mg, K, Ca, Mn and Fe; the main anion is chlorine. A later fluid inclusion assemblage stands out because it displays high salinity (19–23 NaCl

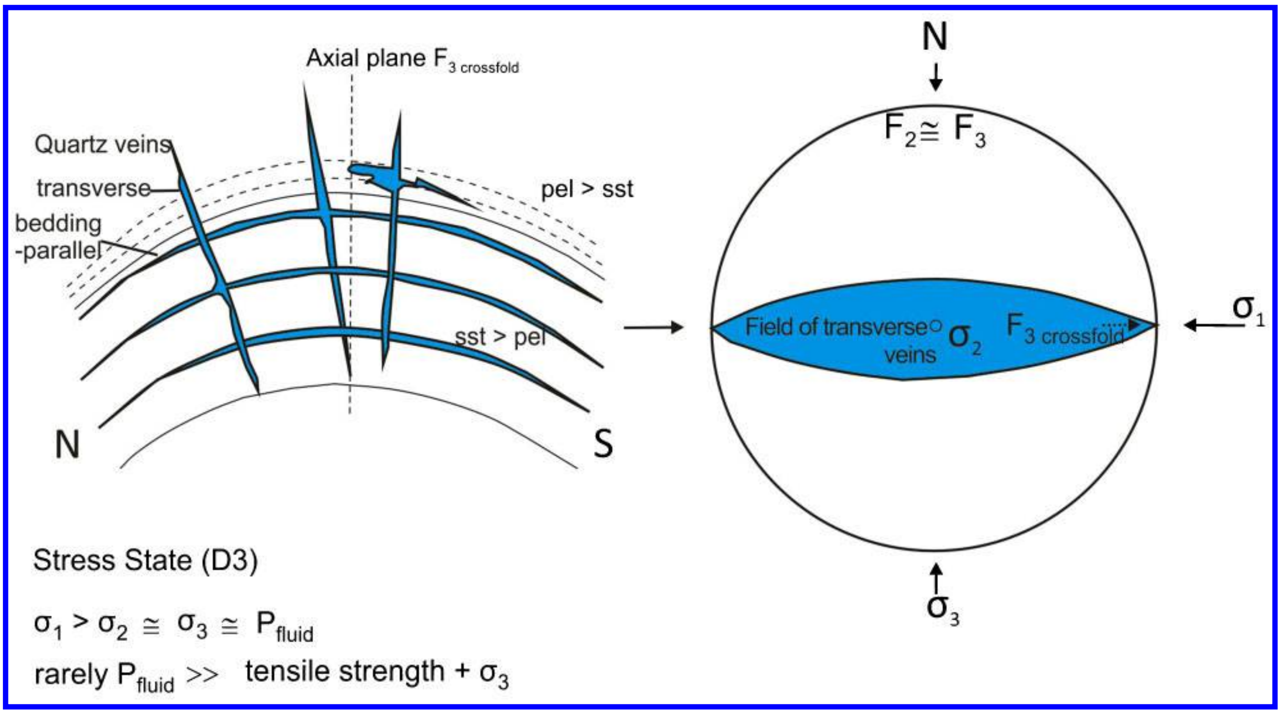

7 Section of anticlinal trap (left), stress field and structural control (equal area projection; right) by pan-Rodinian cross folds of wolframite–quartz veins at Nyakabingo tungsten mine, Rwanda. Host rocks are Mesoproterozoic deep water turbidites; pel – black shales; sst – metapsammites

eq. mass-%) with much $CaCl_2$ (and Fe, Mn), which would be expected for phase (2) replacement of scheelite that necessarily liberates Ca.

$\delta^{18}O$ of hydrothermal fluid (water) in equilibrium with quartz and wolframite (ferberite 1) is ~13 ‰ ('metamorphic') but only 5–6‰ for ferberite 2. The magmatic–hydrothermal signature of the fluids is not preserved; the gas phase demonstrates interaction with organic-rich metasedimentary rocks similar to Rutongo, but more intensive. It is remarkable that the fluid-rock interaction assumed to have caused solubilisation of iron has profoundly shifted $\delta^{18}O$ and δD into the field of organic water (De Clercq, 2012).

Two $^{40}Ar/^{39}Ar$ apparent age spectra of muscovite crystals from tungsten vein fringes yield dates at around 992 and 985 Ma, which confirm the relation to G4 magmatism (De Clercq, 2012). Variably younger ages of muscovite reflect the ubiquitous tectonothermal overprint.

Magmatic–hydrothermal gold

Primary gold mineralisation in the Kibara belt occurs in quartz veins and in fault breccias with sulphides, or after weathering, limonite. At Ruhembe in NW Burundi (Fig. 3 near Kivuvu; Brinckmann *et al.*, 2001, 1994), the auriferous paragenetic sequence evolves from pegmatite (Fig. 8). The hydrothermal deposition begins with an early oxide stage that comprises tourmaline, muscovite, magnetite, cassiterite, wolframite and rutile, followed by refractory gold and sulphides (pyrite and arsenopyrite, and traces of galena, sphalerite and chalcopyrite). Gold is intimately associated with bismuth and bismuthinite. Next, early magnetite and pyrite are replaced by coarse-grained hematite (specularite). Vein fill varies by chemical exchange with immediate host rocks. Veins in metadolerite, for example, that contains much reduced iron, display more ankerite, siderite, ilmenite, magnetite and specularite than veins hosted in metasedimentary rocks. In the Kamituga area (Fig. 3, South Kivu, DRC), gold quartz veins also include graphite, beryl, scheelite and actinolite (Cahen, 1954).

Wide halos of hydrothermal tourmaline ($\pm$rutile) and silica are common. Proximal alteration of metadolerite is characterised by albite, dolomite, pyrite, quartz, arsenopyrite and gold (often at exploitable grades), grading into chlorite–calcite dominated distal rocks. Proximal pelitic metasedimentary rocks and organic-rich shale as at Twangiza display an alteration paragenesis including pyrite, quartz, white mica, arsenopyrite and gold. Veins in quartzite cause marked silicification.

Early fluids precipitating quartz of gold veins in NW-Burundi are characterised by high contents of pure liquid CO_2 and some aqueous fluid with a low to moderate salinity (7–13 mass-% NaCl eq.), and a formation temperature of 360–450°C at 1·7–2 kbar (Brinckmann *et al.*, 2001; Pohl and Günther, 1991). These fluids are NaCl-dominated; they are followed by high salinity Na–Ca–Cl inclusions with halite daughter crystals (23 wt-% NaCl eq.). The absence of N_2 and CH_4 in gold fluids and the high salinity is somewhat different from magmatic–hydrothermal tin and tungsten-depositing fluids but the data base is narrow. Probably, local conditions constrain the evolution. The presence or absence of methane and carbon dioxide in the gas phase, for example, likely reflects interaction of high-temperature magmatic fluids with organic matter of variable maturity in metasedimentary rocks.

U–Pb isotope dating of pegmatites in NW Burundi revealed ages that correlate with G4 granites, whereas disturbed U/Pb ages in zircon ranging from 925–536 Ma, and monazite and rutile ages of 536 ± 5 Ma (Brinckmann *et al.*, 2001) in auriferous Fe–oxide breccias are here not considered to represent formation ages but ubiquitous pan-African rejuvenation already recognised by Cahen *et al.* (1984).

Supergene alteration forms coarse free gold in limonite, often associated with bismutite, scorodite and chalcedony (jasper), limonite-filled boxwork and irregular limonite patches, or coated vugs (Figs. 8, 9A and 9B). This oxide zone gold is the preferred target of both artisanal and industrial mining. It is low (<5 total wt-%) in Ag, Fe, Cu and Hg (Brinckmann *et al.*, 2001, 1994).

Kibaran gold is also extracted from iron-rich horizons of lateritic regolith and predominantly, from alluvial placers. In the Kamituga gold district (Fig. 3), of which the new Twangiza mine is part, around 2·5 Moz alluvial gold have been produced since 1924. Twenty nine gold nuggets weighing over 1 kg each were found in fluvial gravel; the largest weighed 64·8 kg; nuggets had higher gold tenors compared to gold from veins. Also in the Kamituga region, placers buried beneath thick Tertiary basalt have been discovered but not developed (Cahen, 1954). At present, thousands of artisanal miners work young placers and near-surface oxidised ore. The geological background is Kibaran metasedimentary rocks interlaced with Ruzizian (Paleoproterozoic) basement in a fold and thrust belt, and intruded by G4 granite. Some pegmatites carry low tenors of cassiterite and gold, and cut gold-quartz veins or are older (Cahen, 1954). In the region around Twangiza, ill-defined post-1 Ga Itombwe sediments are reported (Fernandez-Alonso *et al.*, 2012, Walemba and Master, 2005).

Twangiza gold mine is located in the Mitumba Mountains about 40 km SSW of Bukavu town (Kivu, DRC; Fig. 3). Ore is hosted within a suite of Kibaran organic carbon-rich mudstones, siltstones, quartzites, a conglomerate (magnetic marker) bed and ill-defined feldspar porphyry sills along the crest of an anticlinal structure. Note that elsewhere, for example in northern Rwanda (Fig. 5) and in NW Burundi in the area of Mabayi (Fig. 3), auriferous veins and breccia zones can occur in synclinal position (Brinckmann *et al.*, 2001). Metamorphism at Twangiza is of very low grade. Small G4 granite outcrops and pegmatites occur in the area and some cassiterite and wolframite was found by colonial prospectors and artisanal miners. Tack *et al.* (2010) published a SHRIMP zircon U–Pb age of 986 Ma for the Kasika G4 granite sampled in the neighbouring Itombwe Plateau. Gold production at Twangiza started in 2011 based on oxidised quartz-limonite ore of 17·9 Mt at 2·3 g/t Au, and sulphide (pyrite–arsenopyrite) ore of 89·6 Mt at 1·5 g/t Au (Banro Corporation, 2013). The ore body is formed by veins that occur in the low-pressure hinge zone of an anticline as bedding-parallel saddle reefs and stockwork bodies. The Twangiza deposit is part of the 210-km-long NE-trending Twangiza–Kamituga–Namoya gold belt, which is currently under exploration by Banro Corporation.

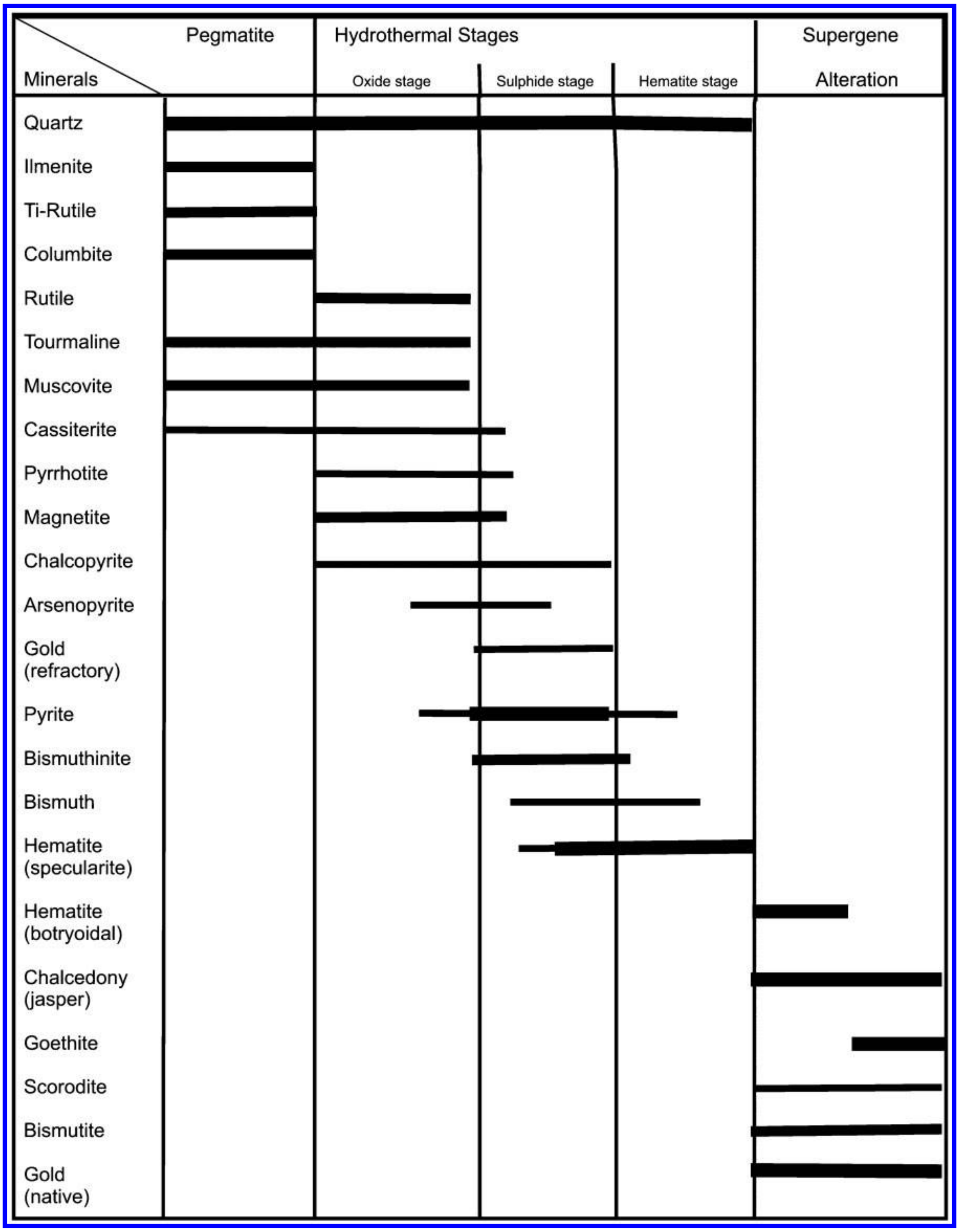

8 Simplified paragenetic sequence of the gold deposit Ruhembe, northwestern Burundi (modified from Brinckmann *et al.*, 2001). The hydrothermal stage evolved from highly fractionated pegmatite. Mafic rocks exerted a strong control on the mineralisation

Towards a metallogenic model

Metallogenic Modelling

Metallogenic modelling requires a full understanding (and ideally, quantification) of the geological processes that drive and control a mineralising system from the source through transport to deposition (Pohl, 2011). The fate of individual elements is traced separately because the diverse geochemical properties of different elements must induce variations. In the early Neoproterozoic (1 Ga) Kibara rare metal and gold province, the elements tin, tungsten, tantalum and gold have the leading economic role. The first three are geochemically classified as lithophile. Gold, in contrast, is highly siderophile (enriched in the Earth's core and to a lesser extent, in its mantle and crust).

For the purpose of this brief sketch, lithophile Sn, W and Ta may be pooled into a group that shares important properties such as the potential extraction from average continental crust by felsic melts (Lehmann,

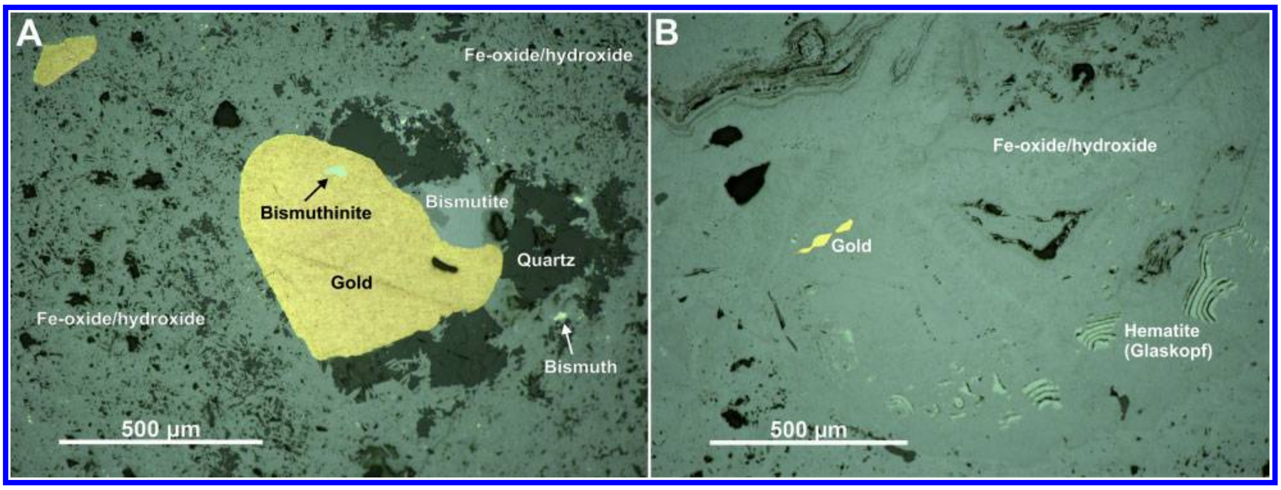

9 (A) Reflected-light photomicrograph of gold (bright) in porous matrix of iron oxide/hydroxide (medium grey) and quartz (dark grey). Black areas are holes. The light grey aggregate intergrown with gold is bismutite (supergene bismuth carbonate). The light inclusion in gold is bismuthinite, and the white spots along the quartz-rich domain are native bismuth. (B) Reflected-light photomicrograph of gold (bright) in iron oxide/hydroxide matrix with relics of hematite in gel-like botryoidal texture. Same location as Fig. 9A

1990), upward transport in rising liquid batches, and, during cooling of an intrusion, the typical incompatible behaviour (enrichment in fractionated residual liquids and fluids compared to the main silicate phases). Tantalum, for example, displays average concentrations of 1 ppm in continental crust; in mineralised LCT pegmatites as at Gatumba, bulk ore has a tenor of >100 ppm (Lehmann *et al.*, 2013). Enrichment processes may be similar, but precipitation mechanisms of Sn, W and Ta are different as exposed in the studies of Kibaran deposit types in the preceding chapter. In contrast to tin and tungsten, tantalum (and niobium) is not soluble in aqueous fluids but crystallises with the pegmatitic melt phase. Tungsten preferentially precipitates from fluids reacting with carbonaceous shale and sandstone, whereas tin enrichment is favoured by opening fractures in brittle rocks combined with alteration of interlayered pelites.

Gold is moderately enriched in the continental crust ($\sim$4 ppb, range 0·05–20 ppb; Pitcairn, 2011), compared to the Earth's primitive mantle ($\sim$0·88 ppb). The S-type character of G4 granites suggests a source made up mainly of metasedimentary rocks. Average gold concentrations of sediments range from 0·1 to 30 ppb, but often decrease during prograde metamorphic devolatilisation (Pitcairn, 2011). The petrogenesis of G4 granites is insufficiently explored regarding the precise redox conditions, sulphur capacity and retention of gold in the liquid phase along its ascent. The transfer of gold into magmatic–hydrothermal fluids seems to be related to a moderate concentration of reduced sulphur that is exposed by the role of sulphide minerals in the gold, tin and tungsten paragenesis. The trapping conditions overlap with the lithophile metals but are different in detail, for example by fluids reacting with reduced iron in mafic host rock. The connection to sulphur and different precipitation controls explain the prevailing detachment of gold from tin and tungsten.

With black shales having a global average gold concentration of 7 ± 1 ppb (Pitcairn, 2011), some gold might have been mobilised by magmatic–hydrothermal fluids reacting with country rocks, similar to sulphur and iron leached from the pyrite-studded black shale in the Rwanda–Uganda tungsten belt. The observed close geochemical connection to rare-element pegmatites, however, is not consistent with the derivation of a significant share of Kibaran gold from metasedimentary rocks.

Data for a quantification of metallogenic processes or process systems such as concentrations, rates and masses involved are not available. Therefore, the brief conceptual metallogenic model sketched here remains qualitative.

Mesoproterozoic foundations of the Kibara Belt insufficiently understood

Among a number of components, a metallogenic model for the Early Neoproterozoic mineralisation in the Central Africa region requires a full understanding of the Mesoproterozoic geological evolution of the Kibara belt. This is, however, still very limited, in spite of recent advances. Among others, gaps concern hard data concerning the relative and absolute timing of orogenic deformation, metamorphism and magmatism across the whole expanse. As a consequence, the overall plate tectonic setting remains uncertain. A possible active continental margin in the Southwest (Kokonyangi *et al.*, 2006, 2005; Kampunzu, 2001) and the steep thermal metamorphic gradients that characterise Kibaran metamorphism suggest the Mesoproterozoic plume modified model of orogenesis in Precambrian eastern Australia (Betts *et al.*, 2009).

Why are tin granites limited to the Mesoproterozoic Kibara Belt?

An improved understanding of the Early Neoproterozoic Sn, Be, Li, Ta, W and Au metallogenesis is also limited in another respect. The superposition of the about 1 Ga granite magmatism and related mineralisation over the whole expanse of the Kibara belt but not beyond would appear to require a link to the processes active during the Mesoproterozoic magmatic and tectonic evolution of the same belt, despite the fact that the two events are separated in time by some 400 million years. In this respect, the Kibaran might be considered as a long lived mobile belt until its final consolidation in the Early

Neoproterozoic. For this reason it is argued that the term Kibaran be retained to describe the belt in its entirety, from initial Mesoproterozoic rifting, sedimentation, folding, metamorphism and batholithic granites to Early Neoproterozoic orogeny and intrusive activity, including the rare and precious metals mineralisation (dissenting with Tack *et al.*, 2010).

To explain the link we speculate that the Mesoproterozoic Kibara fold- and thrust belt provided a lithospheric structure suitable for reactivation ~400 Ma later during pan-Rodinian orogenesis. Coeval with the ~1 Ga Irumide orogeny, this reactivation must have allowed a short-lived thermal disturbance resulting in the G4 granite magmatism. Such flare-up processes of sudden large-scale lower crustal melting are, for instance, known from the Cenozoic Bolivian Andes and the Great Basin of the western USA, and are explained as gravitational instability leading to lithospheric delamination and concomitant asthenospheric upwelling, which provides the heat for melting. The delamination may have been activated by the Tanganyika spur of the Tanzania craton (Fig. 1) indenting into the Kibaran mantle lithosphere and dense mafic lower crust, the latter resulting from extraction of voluminous granitic melt at 1·38 Ga. Like a wedge, the indenter superimposed a N–S directed shortening on the roughly N–S striking and west-vergent folds and thrusts (e.g. Rutongo, Nyakabingo; Fig. 7). An overall compressive stress state was possibly punctuated by short or local extensional events. Post-delamination uplift initiated external and internal molasse sedimentation.

Extraction of pegmatite melt and aqueous fluids from tin granites

A unique exposure between two large Sn–Ta mines in the southern part of the Gatumba district shows banding of microgranite, aplite and pegmatite, and local pockets of muscovite greisen (Figs. 2A, 2B and 4). At the site (150 m in length along a creek) and extending around the creek, scattered quartz and amethyst veining is found. Magmatic bands and veins have the same near-vertical dip and S–N strike as most of the large mineralised pegmatites in the district. To our knowledge, this is the first observation of unaltered rocks clearly exhibiting the passage from granite to mineralised pegmatites in the Kibara belt. Also, the spatial position of the outcrop suggests that the nearby worked pegmatite dykes may set in and widen directly in the metasedimentary rocks above the roof of the granite, or that the vertical distance might be as little as tens of metres. This is different from the schematic zoning model of pegmatites in relation to the roof of the parental granite in which the most evolved pegmatites appear farthest from the granite (Varlamoff, 1972). The outcrop (Fig. 2A) shows differentiated aplite–granite–pegmatite liquids that solidified in fissures of the carapace of a granite cupola. The stress field was determined by the overpressure within the intrusion and tectonic stresses, which controlled the spatial orientation of the pegmatite dykes intruding roof rocks. We suggest that these rocks represent the roof of the specific parental sub-intrusion, which formed the pegmatite field at Gatumba.

Continuity between mineralised pegmatites and hydrothermal mineralisation

Field observation occasionally allows to see a connection between LCT pegmatites and their transition to cassiterite–microcline–quartz veins in the hanging wall as described from the Musha mine in Rwanda (Varlamoff, 1972; Fig. 5) but generally, pegmatitic and vein deposits are clearly separated (Cahen, 1954). In northwestern Burundi, a continuity of hydrothermal mineralisation centred on Sn–Ta-mineralised pegmatites comprises an early high-T oxide stage (anomalous in Sn and W), followed by auriferous sulphides anomalous in bismuth (Fig. 8); in the same area, active artisanal mining works eluvial and alluvial gold placers (Brinckmann *et al.*, 1994). In the Damara belt and the Mozambique belt in southern Africa, low salinity CO_2–H_2O fluids emanating from Li-rich pegmatites are closely linked to gold mineralisation (Banks *et al.*, 2013). These observations might lead to the assumption that all Kibaran hydrothermal ore fluids passed through a pegmatite melt stage. Considering the small size of most pegmatites, however, compared to the metal tonnage in hydrothermal deposits, this is not likely. Another counter argument is the observation, that the Kigali tin granite, which is closely related to the tungsten deposit of Nyakabingo and the tin mining district at Rutongo, displays features of hydrothermal alteration by fluids passing from a deeper level of the solidifying melt body (Günther *et al.*, 1989). With the characteristic disseminated miaroles and/or veinlets of tourmaline and quartz marking many G4 outcrops, the origin of the mineralising fluids directly from solidifying granite is indisputable. Fluid derivation from pegmatite is possible, but a model connecting both mineralised pegmatites and hydrothermal mineralisation to a much larger reservoir is likely, i.e. tapping of residual interstitial liquids and fluids from the solidifying core of a parental intrusion (Lehmann *et al.*, 2013; Pollard and Taylor, 1986).

Is the vein-hosted gold granite-related?

In the past already, the spatial association and mutual co-occurrence of gold, tin and tungsten in the Kibara belt has provoked the assumption that the gold deposits were genetically related to the G4 granites (Cahen, 1954). More recently, additional arguments have been put forward in support of this interpretation:

(i) the co-production of gold and pegmatite-derived columbite and cassiterite from alluvial placers of Northern Burundi (Fig. 8; Brinckmann *et al.*, 1994, 2001);

(ii) the co-production of gold from alluvial placers of hydrothermal cassiterite (Rutongo) and wolframite deposits (Gifurwe); actually at Gifurwe, gold was discovered first and tungsten subsequently;

(iii) often, the structural setting of the Au-veins mimics that of the Sn- and W-vein systems (Twangiza is similar to Nyakabingo; Fig. 7);

(iv) geochemical characteristics of gold mineralisation such as elevated As and Sn concentrations are shared with Sn- and W-veins; high Bi is a link to rare element pegmatites and to parental tin granites;

(v) hydrothermal host rock alteration and vein fill parageneses are very similar for Sn, W and Au;

(vi) although not proving cosanguinity, fluid inclusions data at least allow the assumption of a close relation to magmatic–hydrothermal tin and tungsten.

Ubiquitous rejuvenation of isotope ages

Dating of rocks and minerals reported here confirms that in the Kibara belt, especially along the Western Rift, '*there is much rejuvenation due to later tectono-thermal events*' (Cahen *et al.*, 1984). The SHRIMP U–Pb zircon age of 986±10 Ma (Tack *et al.*, 2010) of tin granite intruding the lower Itombwe succession, however, questions the existence of a 660 Ma Western Rift mobile belt as considered by Cahen *et al.* (1984). Across much of the region, even robust minerals such as columbite and zircon display loss of Pb. Disturbed or reset isotope ages – clearly younger than ~950 and ranging to 500 Ma reflect break-up of Rodinia marked in the Great Lakes region by various 740 to 520 Ma-old carbonatite intrusions (REE mineralised; Lehmann *et al.*, 1994) and related alkaline silica-undersaturated igneous rocks (Tack *et al.*, 1990); and pan-African far-field effects, which are due to the assembly of Gondwana by the East Africa Orogen (EAO; 900–500 Ma) with a collisional climax at 650–550 Ma (Kampunzu, 2001).

Outlook

In the past, the Kibara metal province was systematically investigated by classical prospecting methods and most outcropping ore must have been found. Mineral deposit maps such as the *Carte des Gîtes Minéraux du Zaire* (NN, 2000) display a large number of sites. Because of economic constraints, many lower-grade deposits remained undeveloped. Twangiza gold mine is one example of that category. Regarding the use of modern concepts and technologies, the province is drastically underexplored. There is a considerable potential for the occurrence of Sn–Ta–Be–Li pegmatites and hydrothermal single vein, sheeted vein, saddle vein or stockwork Sn, W, possibly Cu, and Au. Disseminated greisen and replacement Sn (W) deposits are less likely. The next generation of mines will be in hard rock ore below former shallow pits as at Gatumba or new finds below the regolith. Others will occur in deeper roof rocks close to or within hidden cupolas of G4 granites. The potential for a buried equivalent of giant Manono or low-grade high-tonnage apical granite deposits such as Abu Dabbab in Egypt (Küster, 2009) should not be disregarded. The parental sub-intrusion exposed at Gatumba (Figs. 2 and 4) might be a starting point. Placers buried beneath young basalts along the Western Rift are untested. The Eastern margin of the Kibara belt in Tanzania displays one significant gold prospect (west of Mwanza) and a number of rare metal occurrences; this region is considered to have a high gold potential (Kabete *et al.*, 2012).

Because of the generally dense vegetation and thick soil cover, the contribution of remote sensing to mapping and exploration is limited. Geological field work and geophysical methods will play a leading role in improved mapping and discovery. Modern geophysical data, such as airborne gravity, magnetic and radiometric surveys in Rwanda, are only available for limited parts of the whole region. Systematic petrophysical characterisation of mafic sills (metadolerite) and G4 granites is needed for airborne surveys to map their distribution, to locate outcrops and to model buried granite cupolas and elongated ridges. Iron-rich hydrothermal systems (Fig. 8) formed by reaction with the metabasalts are prospective for gold. The morphology of the contact surface between granites and metasedimentary rocks should be mapped to about 2000 m below ground in order to locate favourable structures such as intrusive protuberances. Graphitic schists may mark high temperature contact metamorphism and hydrothermal alteration bodies hosted in black shale. Sulphides can indicate the potential of associated Au or Sn mineralisation.

Geochemical sampling of various materials at all scales will enhance the targeting capability. Useful indicator minerals include white mica and tourmaline that both collect traces of rare alkalis (Be, Li, Rb, Cs) and of tin, tantalum, tungsten and gold. Increasing concentrations of these trace elements are vectors pointing to potential mineralisation. Conspicuous quartz float at the surface, in streams or at the stone line above bedrock suggests dense quartz veining that warrants closer inspection. Highly fractionated and therefore prospective pegmatites are marked by the multi-coloured lithian and Fe-free tourmaline variety called elbaite.

Problems in drilling, sampling and estimating resources and reserves may arise from the nuggety distribution of high-grade ore pockets in all deposit types described; for handling this problem, conceptual principles and practical solutions are available (Dominy and Edgar, 2012). The friable metasomatic wolframite (ferberite 2) requires extreme care, from exploration to recovery of the fines in mine-site ore treatment. Careful reconciliation of grade in place and concentrate yield is advised. Useful equipment for geometallurgical characterisation and delimitation of ore types includes portable X-ray fluorescence analysers.

Although not of imminent practical value for finding ore and somewhat exotic, the investigation of fundamental geological features of the Kibara belt that are at present insufficiently understood, should materially advance scientific understanding and with it, conceptual exploration. Examples include seismic studies of the Kibaran crust and lithosphere, investigations of xenoliths in deeply sourced magmatic rocks, and Sm–Nd and Lu–Hf systematics and zircon ages of G1, G2 and G4 granites across the whole expanse of the Kibara belt. Prospectivity of G4 granites, for example, might be expressed by slight variations of redox and specialisation (Baker *et al.*, 2005), or in a specific range of εNd and εHf values, facilitating the selection of intrusions (or melt batches) with favourable source components.

Acknowledgements

This work is an outcome of the Coltan Environmental Management Project (www.coltan-environmental.org). The project is a research initiative by academics from four countries in the Central Africa Region (Burundi, DR Congo, Rwanda and Uganda, all sharing part of the Kibara tantalum–tin–tungsten–gold metallogenic province) and Germany. The authors gratefully acknowledge financial support by VW Foundation, Hannover. Reviews by S. M. Jowitt and L. J. Robb greatly assisted in improving this paper.

References

Alphamin Resources Corporation, 2013. Bisie project information [online]. Available at: http://alphaminresources.com/ (accessed 2013 August 31).

Baker, T., Pollard, P. J., Mustard, R., Mark, G. and Graham, J. L. 2005. A comparison of granite-related tin, tungsten, and gold-bismuth deposits: implications for exploration. *Soc. Econ. Geol. Nwsl.* **61**, 5–17.

Banks, D. A., MacKenzie, C. J. and Yardley, B. W. D. 2013. Pegmatite fluids as a source for gold mineralisation. *Appl. Earth Sci.*, **121**, 214–215.

Banro Corporation, 2013. Twangiza project information. [online] Available at: http://www.banro.com/ (accessed 2013 August 31).

Bassot, J.-P. and Morio, M. 1989. Morphologie et mise en place de la pegmatite kibarienne à Sn, Nb, Li de Manono (Zaire). *Chronique Rech. Minières*, **496**, 41–56.

Baudin, B., Zigirababili, J., Ziserman, A. and Petricec, V. 1982. Carte des Gîtes Minéraux du Rwanda 1 : 250·000, Kigali, Ministère des Ressources Minières, République Rwandaise.

Betts, P. G., Giles, D., Foden, J., Schaefer, B. F., Mark, G., Pankhurst, M. J., Forbes, C. J., Chalmers, N. C. and Hills, Q. 2009. Mesoproterozoic plume-modified orogenesis in eastern Precambrian Australia. *Tectonics*, **28**, 1–28.

Brinckmann, J., Lehmann, B., Hein, U., Höhndorf, A., Mussallam, K., Weiser, T. and Timm, F. 2001. La géologie et la minéralisation primaire de l'or de la chaîne Kibarienne, nord-ouest du Burundi, Afrique orientale. *Geol. Jb.* D, **101**, 3–195.

Brinckmann, J., Lehmann, B. and Timm, F. 1994. Proterozoic gold mineralisation in NW Burundi. *Ore Geol. Rev.*, **9**, 85–103.

Burke, K. and Gunnel, Y. 2008. The African erosion surface: A continental-scale synthesis of geomorphology, tectonics, and environmental change over the past 180 million years. *Geol. Soc. Am. Mem.*, 201.

Cahen, L. 1954. Géologie du Congo Belge. Liège, Vaillant-Carmanne.

Cahen, L., Snelling, N. J., Delhal, J. and Vail, J. R. 1984. The geochronology and evolution of Africa. Oxford, Clarendon.

De Clercq, F. 2012. Metallogenesis of Sn and W vein-type deposits in the Karagwe-Ankole belt (Rwanda), PhD thesis, KU Leuven [online]. Available at: https://lirias.kuleuven.be/handle/123456789/360497 (accessed 2013 August 31).

De Waele, B., Johnson, S. P. and Pisarevsky, S. A. 2008. Palaeoproterozoic to Neoproterozoic growth and evolution of the eastern Congo Craton: Its role in the Rodinia puzzle. *Precambrian Res.*, **160**, 127–141.

De Waele, B., Wingate, M. T. D., Fitzsimons, I. C. W. and Mapani, B. S. E. 2003. Untying the Kibaran knot: A reassessment of Mesoproterozoic correlations in southern Africa based on SHRIMP U-Pb data from the Irumide belt. *Geology*, **31**, 509–512.

Dewaele, S., Henjes-Kunst, F. and Melcher, F. 2011. Late Neoproterozoic overprinting of the cassiterite and columbite-tantalite bearing pegmatites of the Gatumba area, Rwanda (Central Africa). *J. Afr. Earth Sci.*, **61**, 10–26.

Dominy, S. C and Edgar, W. B. 2012. Approaches to reporting grade uncertainty in high nugget gold veins. *Appl. Earth Sci.*, **121**, 29–42.

Fernandez-Alonso, M., Cutten, H., De Waele, B., Tack, L., Tahon, A., Baudet, D. and Barritt, S. D. 2012. The Mesoproterozoic Karagwe-Ankole Belt (formerly the NE Kibara Belt): The result of prolonged extensional intracratonic basin development punctuated by two shortlived far-field compressional events. *Precambrian Res.*, **216–219**, 63–86.

Fernandez-Alonso, M., Laghmouch, M., Tack, L. and Tahon, A. 2007. Geological Map of the Mesoproterozoic Northeastern Kibara belt. Series '1/500 000, Tervuren, Royal museum for central Africa (RMCA).

Günther, M. and Ngulube, A. 1992. The lithium-pegmatite at Manono, Zaire. *IGCP 255 Nwsl. /Bull.*, **4**, 91–99.

Günther, M., Dulski, P., Lavreau, J., Lehmann, B., Möller, P. and Pohl, W. 1989. The Kibaran tin granites: hydrothermal alteration versus plate tectonic setting. *IGCP 255 Nwsl. /Bull.*, **2**, 21–27.

Hulsbosch, N., Hertogen, J., André, L., Dewaele, S. and Muchez, P. 2013. Chemical fractionation of the Nb-Ta-Sn mineralised pegmatites of the Gatumba area (Rwanda). *Appl. Earth Sci.*, **121**, 194–195.

Kabete, J. M., Groves, D. I., McNaughton, M. J. and Mruma, A. H. 2012. A new tectonic and temporal framework for the Tanzanian Shield: Implications for gold metallogeny and undiscovered endowment. *Ore Geol. Rev.*, **48**, 88–124.

Kampunzu, A. B. 2001. Assembly and break-up of Rodinia – no link with Gondwana assembly. *Gondwana Res.*, **4**, (4), 647–650.

Kokonyangi, J. W., Kampunzu, A. B., Armstrong, R., Makoto Arima, Masaru Yoshida and Takamoto Okudaira, 2007. U-Pb SHRIMP dating of detrital zircons from the Nzilo Group (Kibaran Belt): implications for the source of sediments and Mesoproterozoic evolution of Central Africa. *J. Geol.*, **115**, 99–113.

Kokonyangi, J. W., Kampunzu, A. B., Armstrong, R., Yoshida, M., Okudaira, T., Arima, M. and Ngulube, D. A. 2006. The Mesoproterozoic Kibaride belt (Katanga, SE D. R. Congo). *J. Afr. Earth Sci.*, **46**, 1–35.

Kokonyangi, J. W., Kampunzu, A. B., Poujol, M., Okudaira, T., Yoshida, M. and Shabeer, K. P. 2005. Petrology and geochronology of Mesoproterozoic mafic–intermediate plutonic rocks from Mitwaba (D. R. Congo): implications for the evolution of the Kibaran belt in central Africa. Geol. Mag., **142**, 109–130.

Küster, D. 2009. Granitoid-hosted Ta mineralization in the Arabian–Nubian Shield: Ore deposit types, tectono-metallogenetic setting and petrogenetic framework. *Ore Geol. Rev.*, **35**, 68–86.

Lang, J. R. and Baker, T. 2001. Intrusion-related gold systems: the present level of understanding. *Miner. Depos.*, **36**, 477–489.

Lehmann, B. 1990. Metallogeny of tin, Berlin, Springer.

Lehmann, B., Halder, S., Ruzindana Munana, J., Ngizimana, Jean de la Paix and Biryabarema, M. 2013. The geochemical signature of rare-metal pegmatites in Central Africa: Magmatic rocks in the Gatumba tin-tantalum mining district, Rwanda, accepted for print, *J. Geochem. Explor*.

Lehmann, B., Dietrich, A. and Heinhorst, J. 2000. Boron in the Bolivian tin belt. *Miner. Depos.*, **35**, 223–232.

Lehmann, B., Nakai, S. I., Höhndorf, A., Brinckmann, J., Dulski, P., Hein, U. F. and Masuda, A. 1994. REE mineralization at Gakara, Burundi: Evidence for anomalous upper mantle in the western Rift Valley. *Geochim. Cosmochim. Acta*, **58**, 985–992.

Lehmann, B. and Lavreau, J. 1988. Geochemistry of the tin granites from Kivu (Zaire), Rwanda and Burundi. *IGCP 255 Nwsl. /Bull.*, **1**, 43–46.

Li, Z. X., Bogdanova, S. V., Collins, A. S., Davidson, A., De Waele, B., Ernst, R. E., *et al.* 2008. Assembly, configuration, and break-up history of Rodinia: A synthesis, *Precambrian Res.* **160**, 179–210.

Maier, W. D., Barnes, S.-J., Bandyayera, D., Livesey, T., Li, C. and Ripley, E. 2008. Early Kibaran rift-related mafic–ultramafic magmatism in western Tanzania and Burundi: Petrogenesis and ore potential of the Kapalagulu and Musongati layered intrusions. *Lithos*, **101**, 24–53.

Maier, W. D., Peltonen, P. and Livesey, T. 2007. The ages of the Kabanga North and Kapalagulu intrusions, western Tanzania: a reconnaissance study. *Econ. Geol.*, **102**, 147–154.

NN, 2000. *Carte des Gîtes Minéraux du Zaire 1 : 2 000 000*. Orléans, BRGM; Kinshasa, Direction du Service Géologique, République du Zaire.

Pitcairn, I. 2011. Background concentrations of gold in different rock types. *Appl. Earth Sci.*, **120**, 31–38.

Pohl, W. L. 2011. Economic geology, principles and practice: metals, minerals, coal and hydrocarbons – an introduction to formation and sustainable exploitation of mineral deposits, Oxford, Wiley-Blackwell.

Pohl, W. 1994. Metallogeny of the northeastern Kibara belt, Central Africa - recent perspectives. *Ore Geol. Rev.*, **9**, 105–130.

Pohl, W. 1987. Metallogeny of the northeastern Kibara belt, Central Africa. *Geol. J.*, **22**, 103–119.

Pohl, W. and Günther, M. A. 1991. The origin of Kibaran (late Mid-Proterozoic) tin, tungsten and gold quartz vein deposits in Central Africa: a fluid inclusions study. *Miner. Depos.*, **26**, 51–59.

Pohl, W. and Hadoto, D. P. M. 1990. Granite-related Kibaran gold mineralization at Mashonga, Bushenyi district (SW Uganda). *IGCP 255 Nwsl. /Bull.*, **3**, 61–67.

Pollard, P. J. and Taylor, R. G. 1986. Progressive evolution of alteration and tin mineralization: controls by interstitial permeability and fracture-related tapping of magmatic fluid reservoirs in tin granites. *Econ. Geol.*, **81**, 1795–1800.

RMCA (Royal Museum for Central Africa), 2005a. The mineral occurrences map of the Republique Democratique du Congo. Includes Geological Map 1 : 2 000 000, Tervuren, CD ROM.

RMCA (Royal Museum for Central Africa), 2005b. Regular maps (space maps) of Kivu and Maniema (DRC). Scale 1 : 200 000, Tervuren.

Romer, R. L. and Lehmann, B. 1995. U-Pb columbite age of Neoproterozoic Ta-Nb mineralization in Burundi. *Econ. Geol.*, **90**, 2303–2309.

Tack, L., Wingate, M. T. D., De Waele, B., Meert, J., Belousova, E., Griffin, B., Tahon, A. and Fernandez-Alonso, M. 2010. The 1375 Ma 'Kibaran event' in Central Africa: Prominent emplacement of bimodal magmatism under extensional regime. *Precambrian Res.*, **180**, 63–84.

Tack, L., De Paepe, P., Liégeois, J. P., Nimpagaritse, G., Ntungicimpaye, A. and Midende, G. 1990. Late Kibaran magmatism in Burundi. *J. Afr. Earth Sci.*, **10**, 733–738.

Thomas, R. J., Bühmann, D., Bullen, W. D., Scogings, A. J. and De Bruin, D. 1994. Unusual spodumene pegmatites from the Late Kibaran of southern Natal, South Africa. *Ore Geol. Rev.*, **9**, 161–182.

Varlamoff, N. 1972. Central and West African rare metal granitic pegmatites, related aplites, quartz veins and mineral deposits. *Miner. Depos.*, **7**, 202–216.

Walemba, K. M. A. and Master, S. 2005. Neoproterozoic diamictites from the Itombwe Synclinorium, Kivu Province, Democratic Republic of Congo: Palaeoclimatic significance and regional correlations. *J. Afr. Earth Sci.*, **42**, 200–210.

Ziserman, A., Zigirababili, J., Petricec, V. and Baudin, B. 1983. Données sur la métallogénie du Rwanda. Enseignements tirés de la carte des gîtes minéraux. *Chronique Rech. Minières*, **471**, 31–40.